

Electronic Supplementary information

**Co(II)-porphyrins decorated carbon nanotubes as catalysts for oxygen
reduction reactions: An approach for fuel cell improvement†**

*Piyush Kumar Sonkar¹, Kamal Prakash², Mamta Yadav¹, Vellaichamy Ganesan*¹, Muniappan
Sankar², Rupali Gupta¹, Dharmendra Kumar Yadav¹*

¹Department of Chemistry, Institute of Science

Banaras Hindu University, Varanasi-221 005, UP, India

Telephone: + 91-542-6701609; Fax: + 91-542-2368127

Email: velganesh@yahoo.com and velgan@bhu.ac.in

²Department of Chemistry, Indian Institute of Technology Roorkee,
Roorkee-247667, Uttarakhand, India

* Corresponding author

Section S1

Conversion of observed experimental potential to reversible hydrogen electrode, RHE scale

The experimentally observed potentials against Ag/AgCl or saturated calomel electrode, SCE are converted to the reversible hydrogen electrode (RHE) scale according to the Nernst equation [SR1-SR3]:

$$E_{RHE} = E_{Ag/AgCl} + 0.059pH + E^0_{Ag/AgCl} \quad (1)$$

$$E_{RHE} = E_{SCE} + 0.059pH + E^0_{SCE} \quad (2)$$

where $E_{Ag/AgCl}$ is the experimentally measured potential against Ag/AgCl reference electrode and $E^0_{Ag/AgCl}$ is 0.199 V at 25 °C. Similarly, E_{SCE} is the experimentally measured potential against SCE reference and E^0_{SCE} is 0.241 at 25 °C.

References

- [SR1] G. Ferrero, K. Preuss, A. Fuentes, M. Sevilla and M.-M. Titirici, *Journal of Materials Chemistry A*, 2016, **4**, 2581-2589.
- [SR2] A. J. Bard, L. R. Faulkner, J. Leddy and C. G. Zoski, *Electrochemical methods: fundamentals and applications*, Wiley New York, 1980.
- [SR3] D. Y. Chung, S. W. Jun, G. Yoon, S. G. Kwon, D. Y. Shin, P. Seo, J. M. Yoo, H. Shin, Y.-H. Chung and H. Kim, *Journal of the American Chemical Society*, 2015, **137**, 15478-15485.

Table S1 Composition of MWCNT-CoTHPP, MWCNT-CoTCPP and MWCNT-CoTPP in different weight ratios and amount of metal complex adsorbed.

Name of the sample (MWCNT (in mg) : metal complex (in mmoles))	Initial composition added		Final composition after adsorption		
	MWCNT (mg)	Cobalt porphyrin (mg)	% N (obtained from elemental analysis)	N calculated (mg)	Cobalt porphyrin calculated (mg)
MWCNT-CoTHPP (10:0.02)	10	14.70	1.11	0.266	2.94
MWCNT-CoTPP (10:0.02)	10	13.42	4.10	1.428	10.065
MWCNT-CoTCPP (10:0.02)	10	16.94	2.12	0.574	8.47
MWCNT-CoTHPP (10:0.01)	10	07.35	1.07	0.184	2.205
MWCNT-CoTPP (10:0.01)	10	06.71	4.14	1.442	6.70
MWCNT-CoTCPP (10:0.01)	10	08.47	2.03	0.378	5.929
MWCNT-CoTHPP (10:0.005)	10	03.68	0.65	0.088	1.1025
MWCNT-CoTPP (10:0.005)	10	03.35	1.19	0.1596	1.878
MWCNT-CoTCPP (10:0.005)	10	04.24	0.77	0.1092	1.6093
MWCNT (10:0.00)	10	00.00	0.00	0.00	0.000
MWCNT-CoTPP (10:0.001)	10	0.671	0.56	0.084	0.671
MWCNT-CoTHPP (10:0.001)	10	0.735	0.52	0.098	0.5145
MWCNT-CoTCPP (10:0.001)	10	0.847	0.41	0.126	0.5929

Fig. S1 IR spectra of the (a) MWCNT, (b) CoTHPP (c) MWCNT-CoTHPP, (d) CoTCPP, (e) MWCNT-CoTCPP, (f) CoTPP, (g) MWCNT-CoTPP with the KBr pallets.

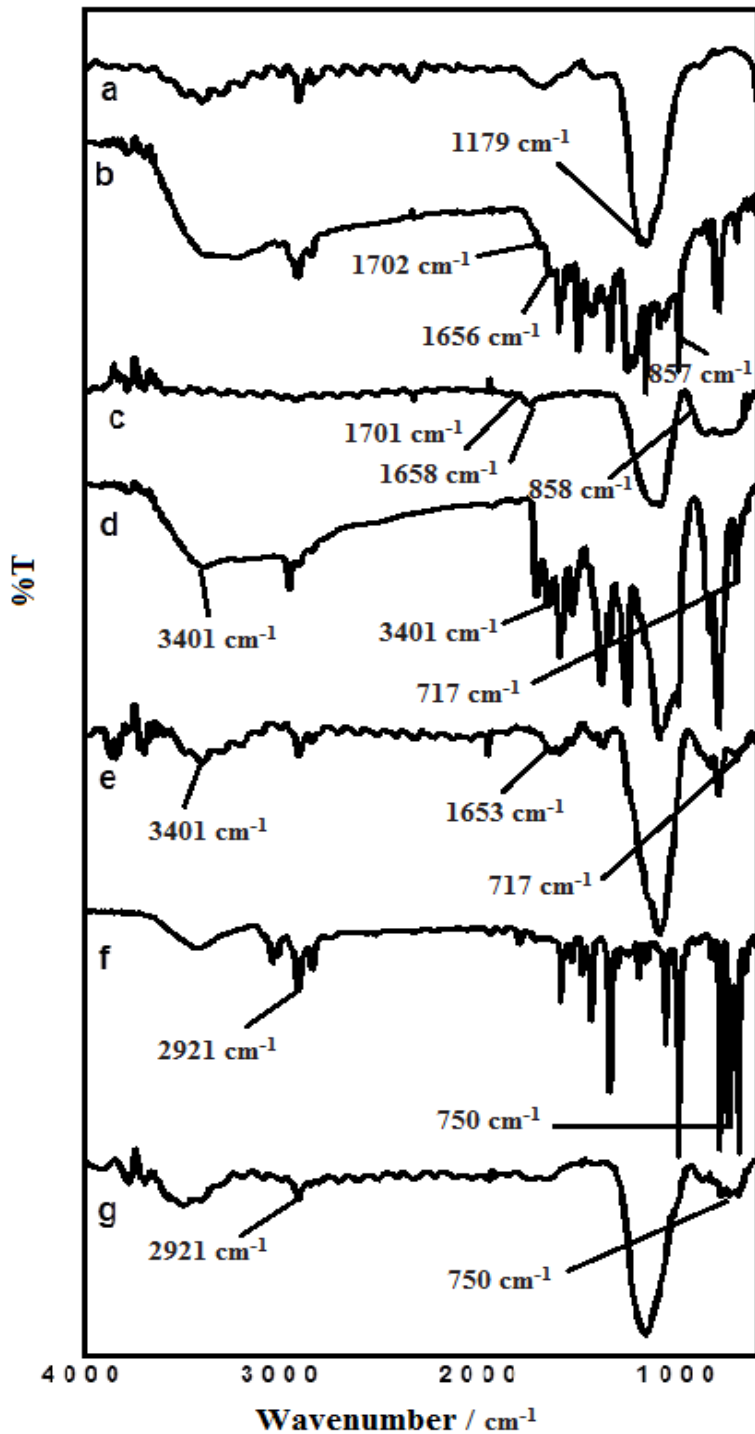


Fig. S2(A) EDAX mapping of MWCNT-CoTHPP composite showing the element distribution in the material.

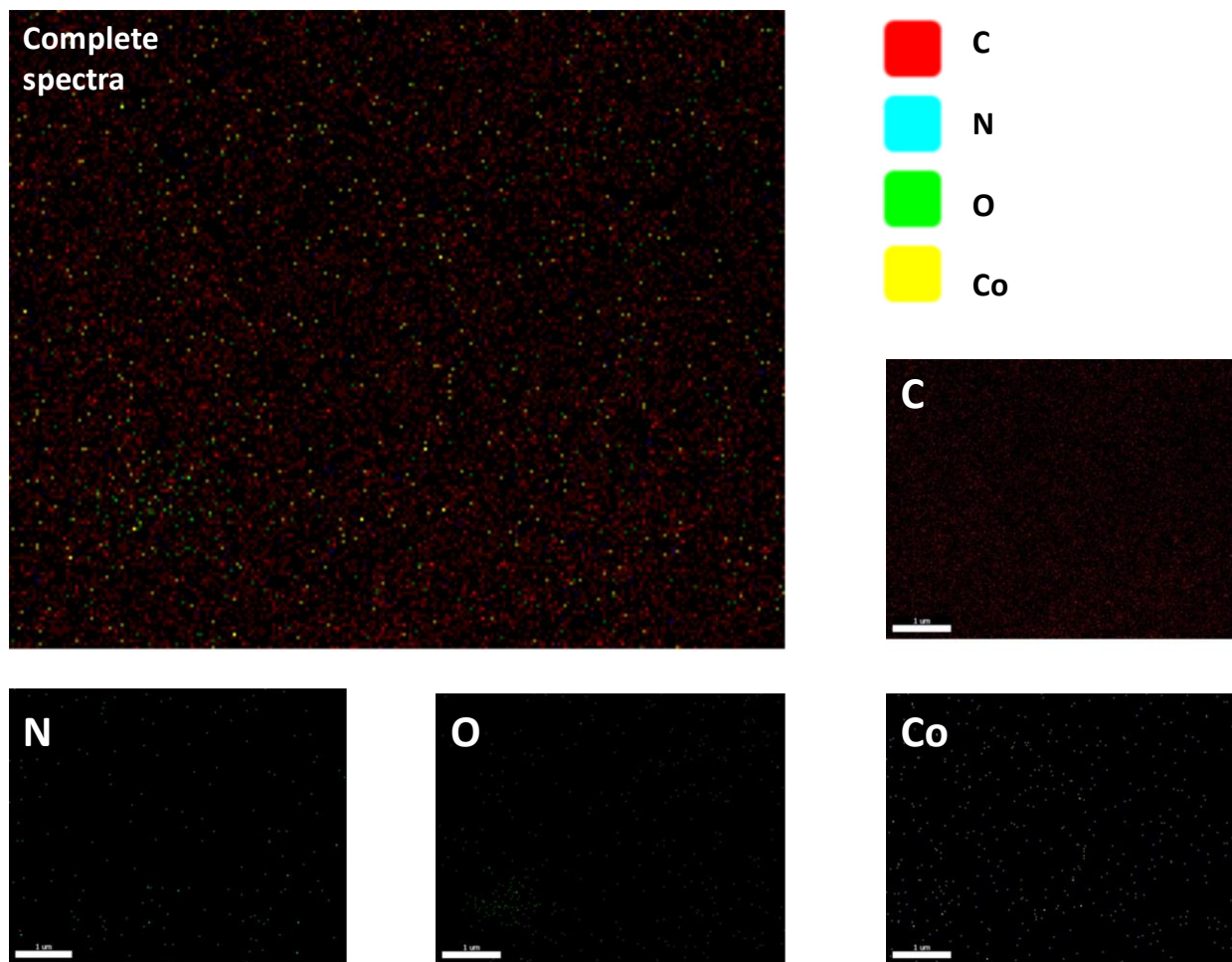


Fig. S2(B) EDAX mapping of MWCNT-CoTCPP composite showing the element distribution in the material.

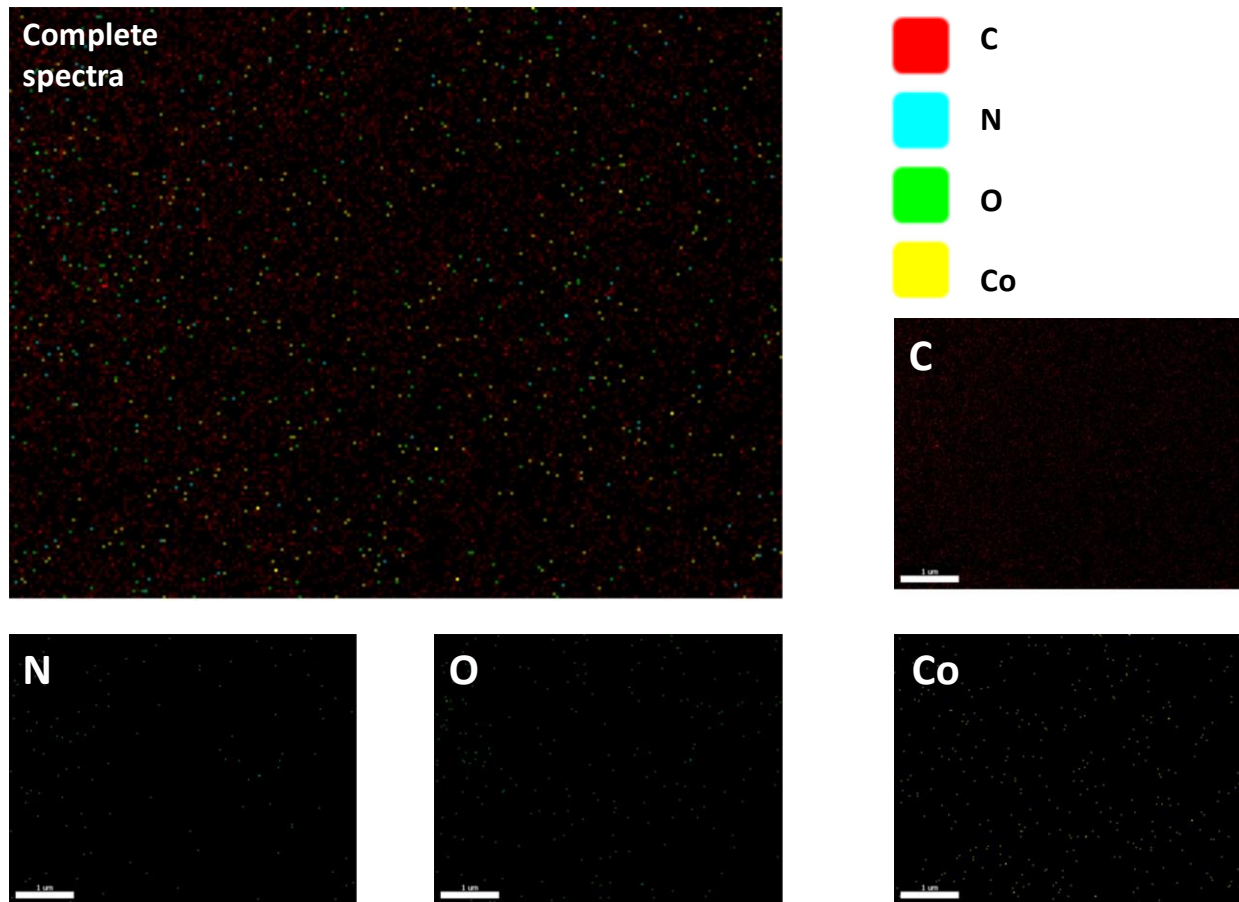


Fig. S2(C) EDAX mapping of MWCNT-CoTPP composite showing the elemental distribution in the material.

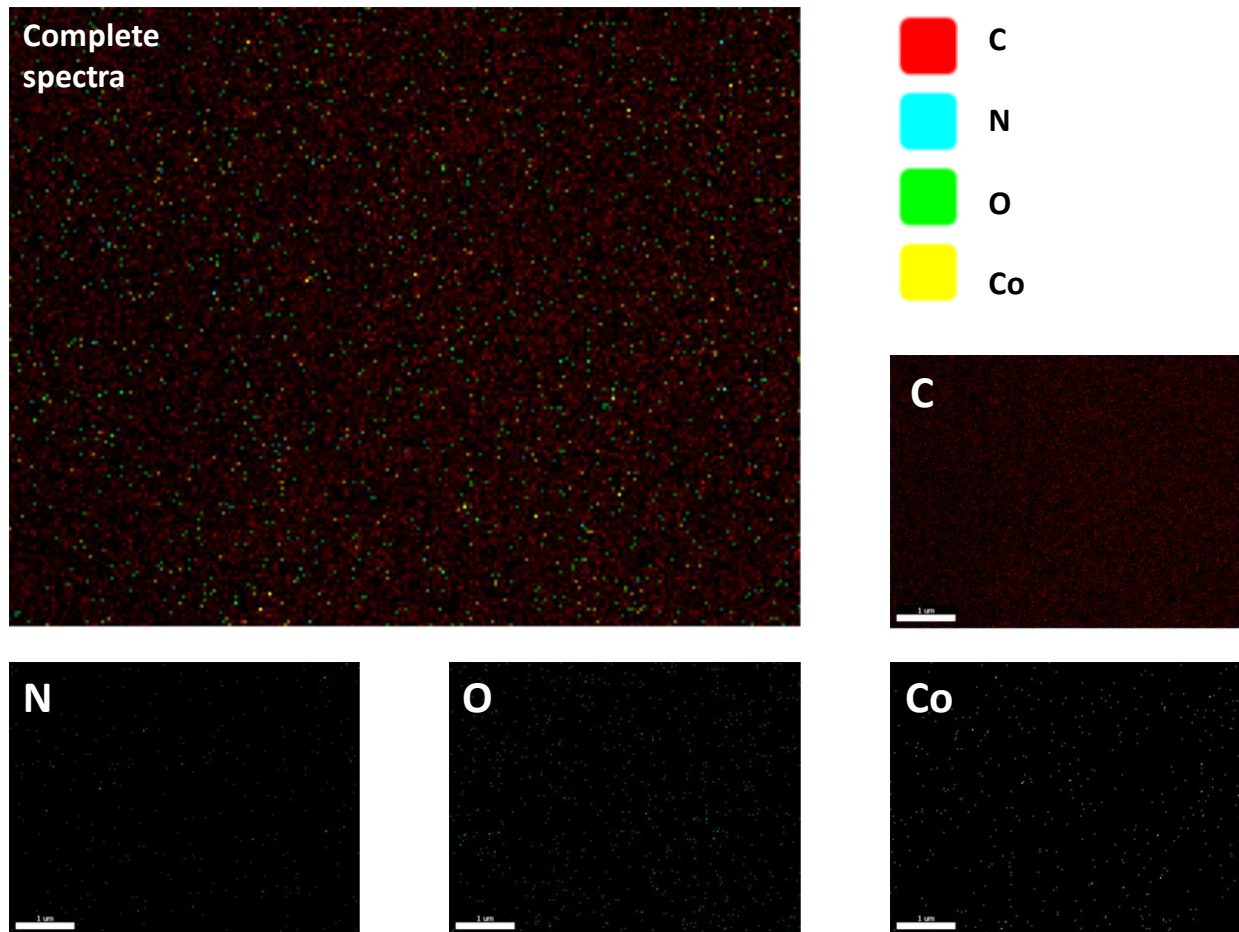


Fig. S3 Plot showing the nitrogen adsorption with MWCNT, MWCNT-CoTHPP, MWCNT-CoTCPP and MWCNT-CoTPP materials.

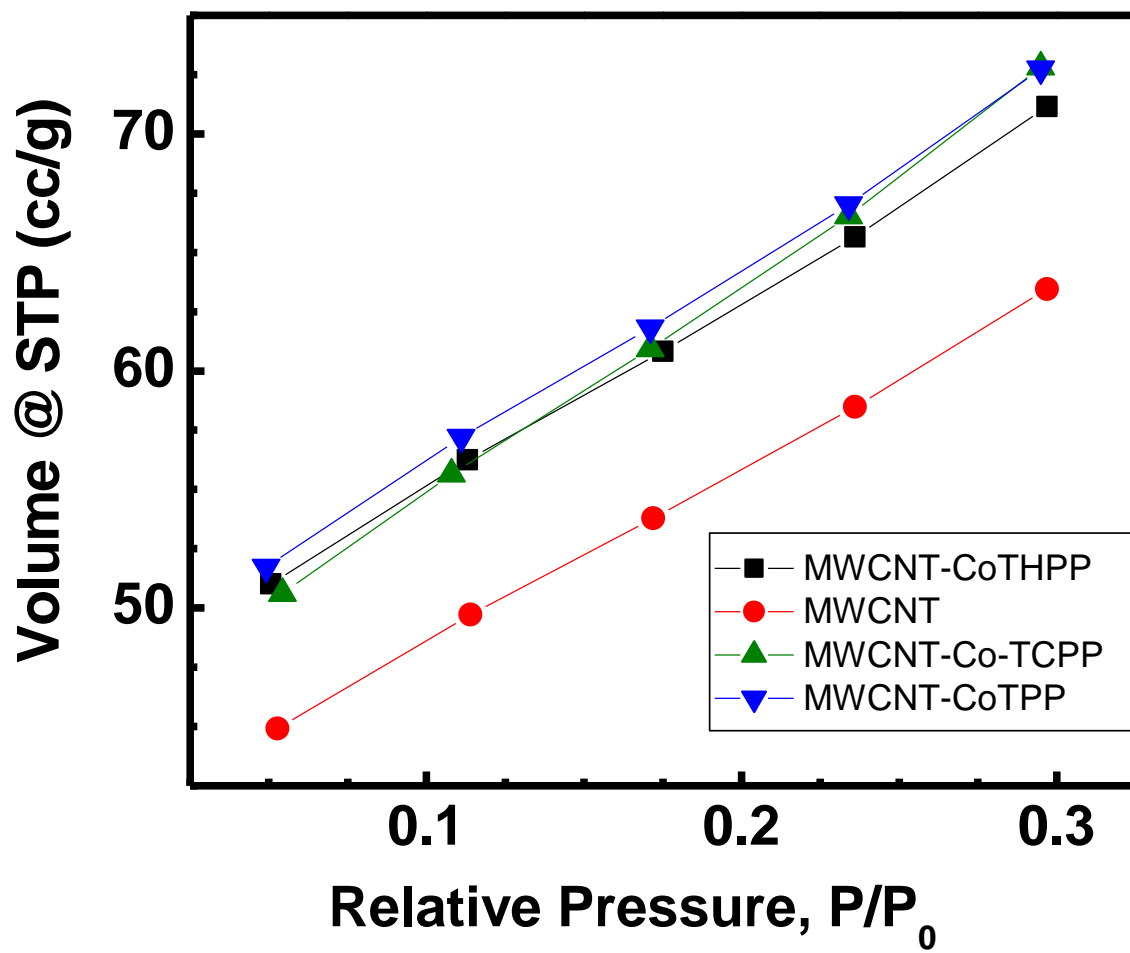


Fig. S4 CV response of GC/MWCNT-CoTHPP (a), GC/MWCNT-CoTCPP (b) and GC/MWCNT-CoTPP (c) at different scan rates 20, 50, 75, 100, 200, 300, 400, 500 mVs⁻¹ in 0.1 M HClO₄. (a'-c') represents the respective plot of anodic (I_{pa}) and cathodic (I_{pc}) peak current vs square root of scan rate.

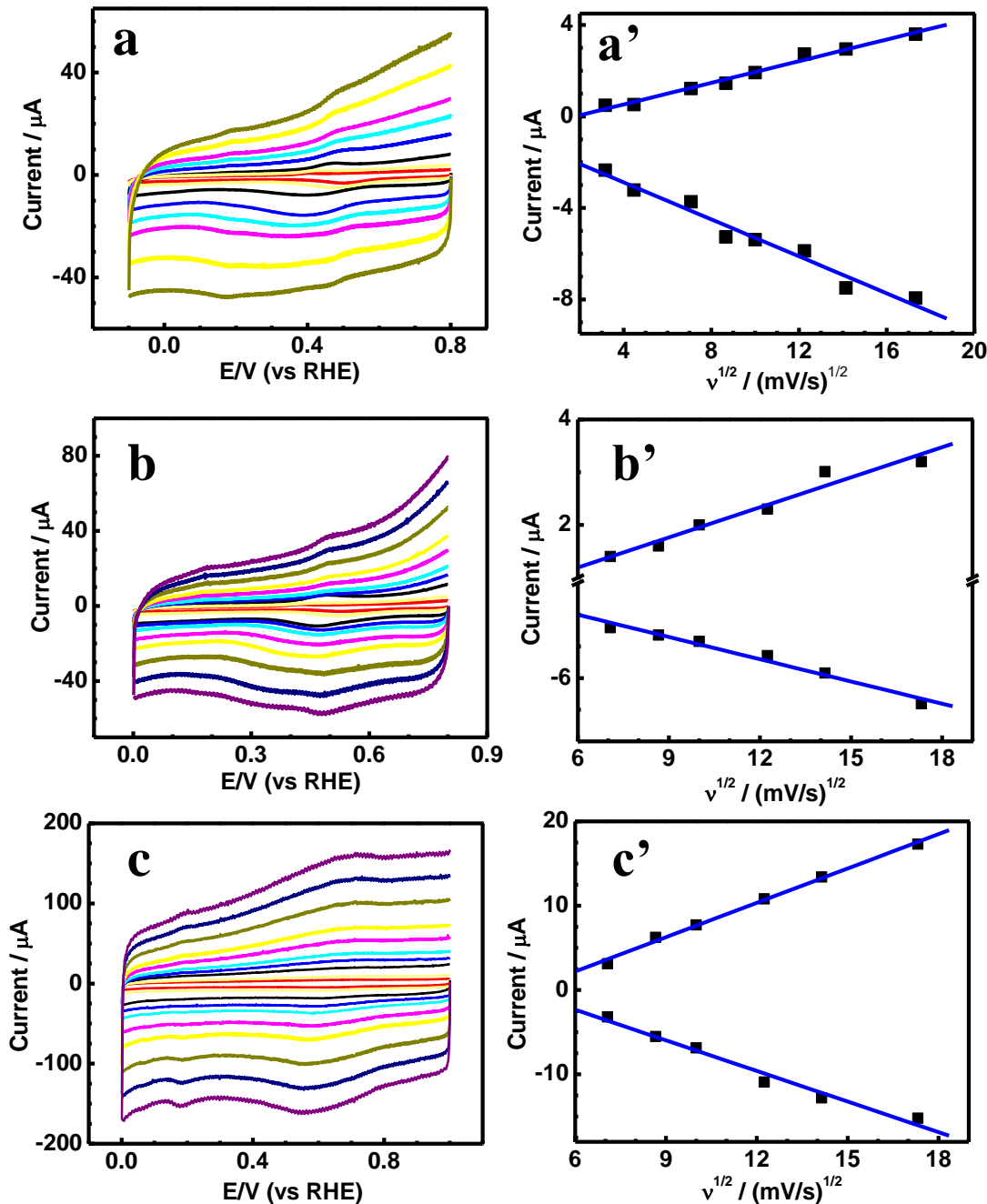


Fig. S5 CV response of GC/MWCNT-CoTHPP (a, a' and a''), GC/MWCNT-CoTCPP (b, b' and b''), GC/MWCNT-CoTPP (c, c' and c''), GC/MWCNT (d, d' and d'') and GC/Pt-C (e, e' and e'') electrodes in 0.1 M HClO₄ (a to e), 0.1 M PBS, pH 7.0 (a' to e') and in 0.1 M KOH (a'' to e'') solutions saturated with either nitrogen (dashed line) or oxygen (solid line).

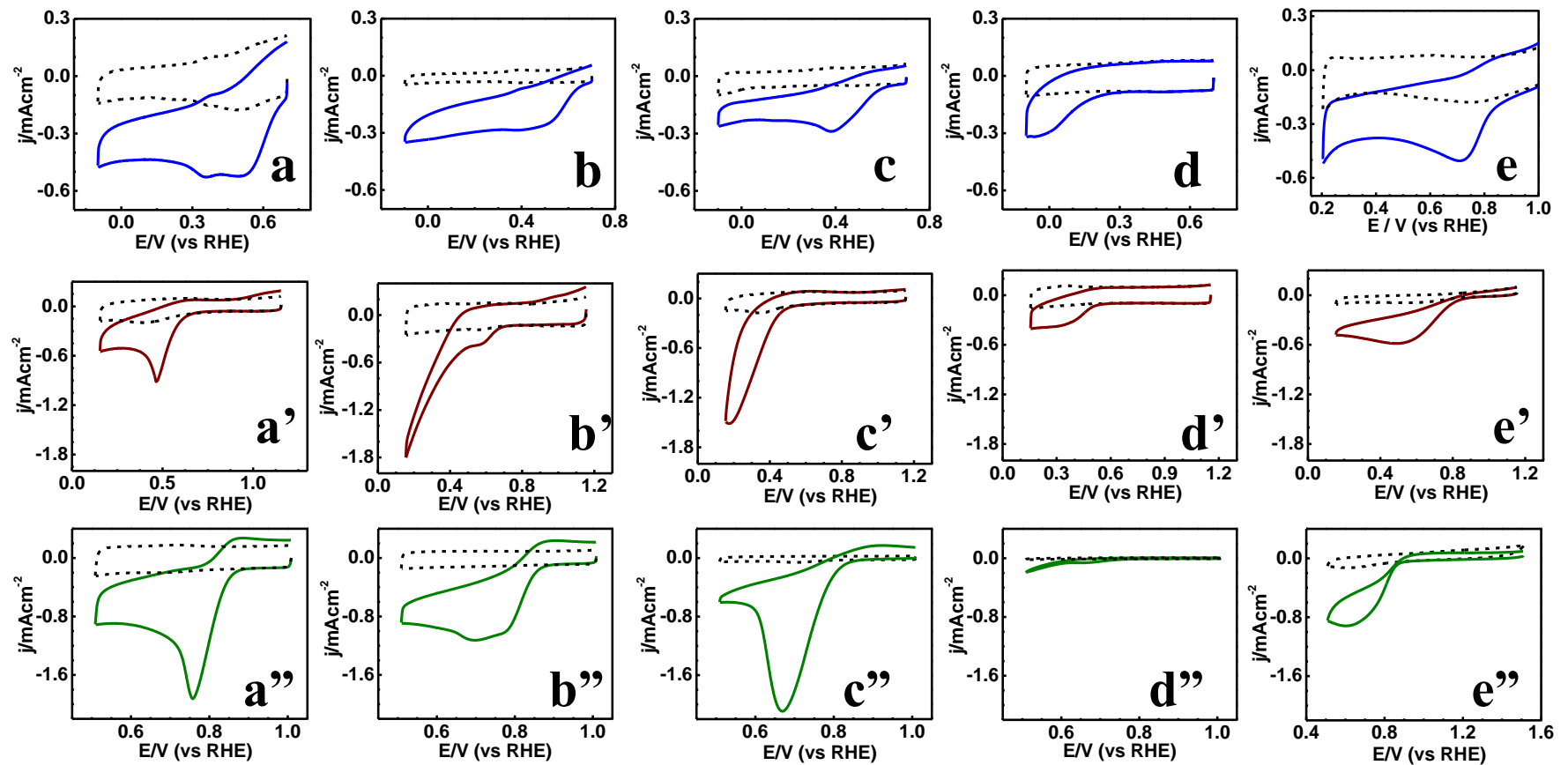


Fig. S6 CV response of different cobalt porphyrins films based electrodes in 0.1 M HClO₄ (a), 0.1 M PBS pH 7.0 (b) and 0.1 M KOH (c) in oxygen saturated condition with the scan rate of 20 mVs⁻¹.

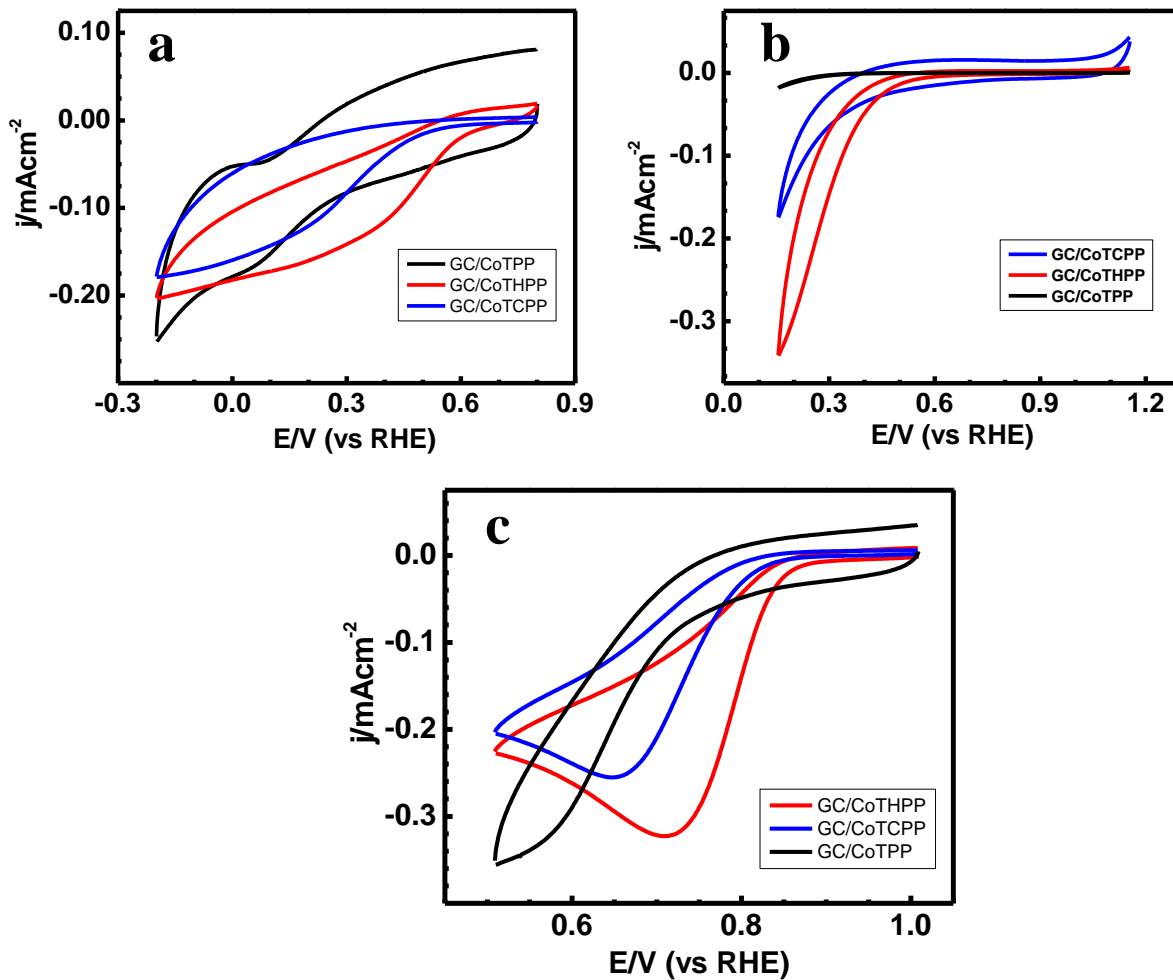


Fig. S7 CV response in 0.1 M KCl with 10.0 mM $\text{K}_3[\text{Fe}(\text{CN})_6]/\text{K}_4[\text{Fe}(\text{CN})_6]$ (1:1) for active surface area determination. Where, a, b, c and d stands for GC/MWCNT-CoTHPP, GC/MWCNT-CoTCPP, GC/MWCNT-CoTPP, and GC/MWCNT, respectively.

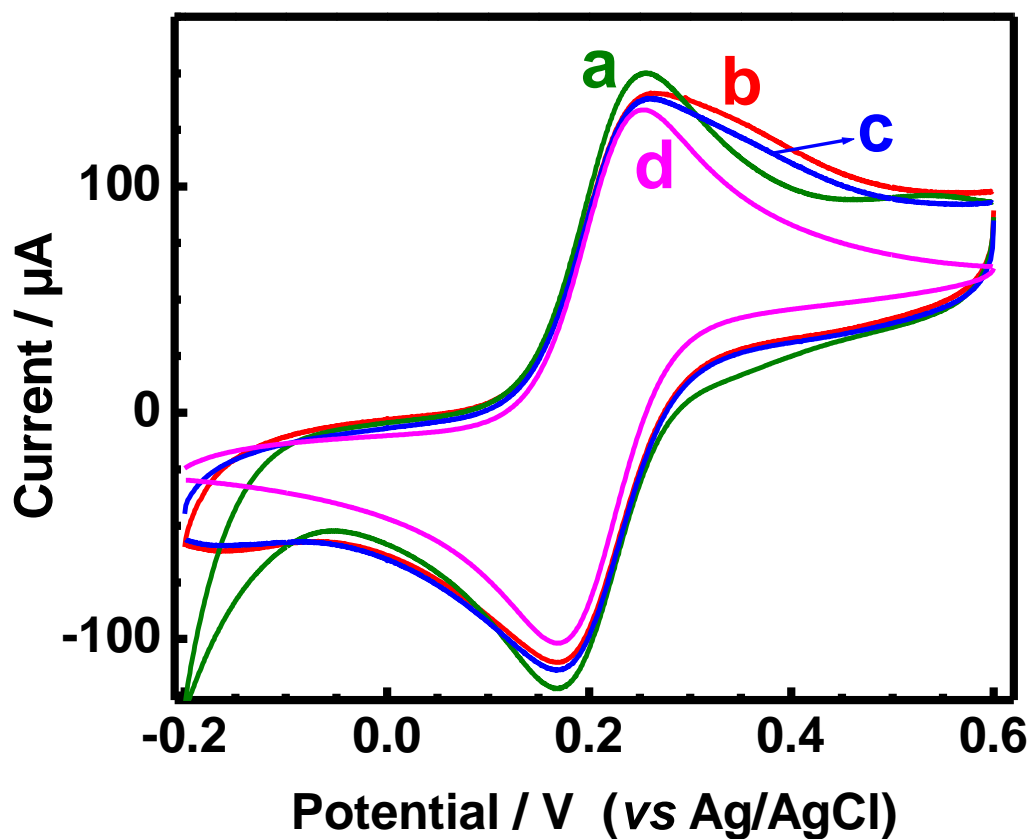


Fig. S8 Current-potential curves at different rotation rates in 0.1 PBS pH 7.0 at a scan rate of 10 mVs⁻¹ in oxygen saturated condition (A-C) and the respective Koutecky-Levich plots (D-F) for GC/MWCNT-CoTHPP (A, D), GC/MWCNT-CoTCPP (B, E) and GC/MWCNT-CoTPP (C, F).

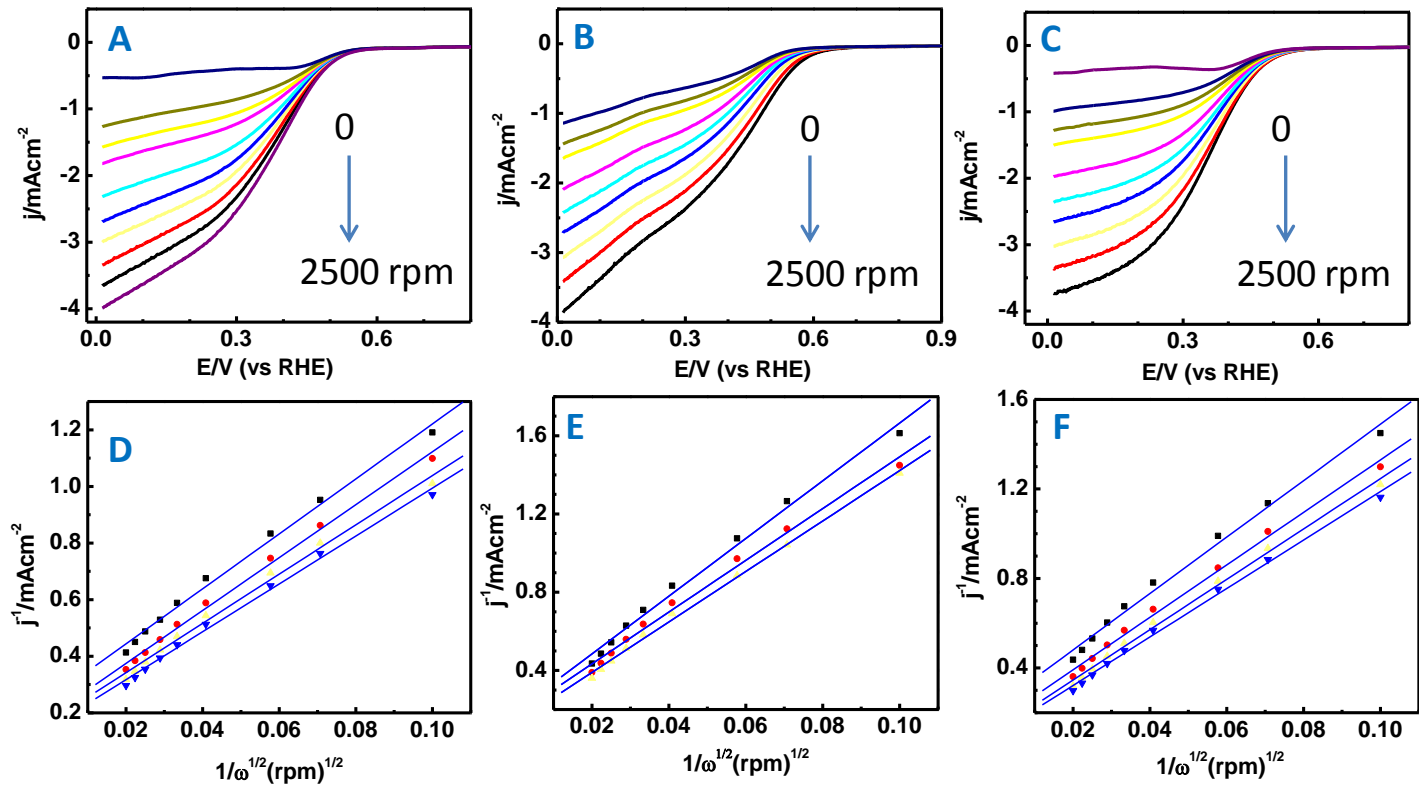


Fig. S9

Current-potential curves at different rotation rates in 0.1 M KOH at a scan rate of 10 mVs⁻¹ in oxygen saturated condition (A-C) and the respective Koutecky-Levich plots (D-F) for GC/MWCNT-CoTHPP (A, D), GC/MWCNT-CoTCPP (B, E) and GC/MWCNT-CoTPP (C, F).

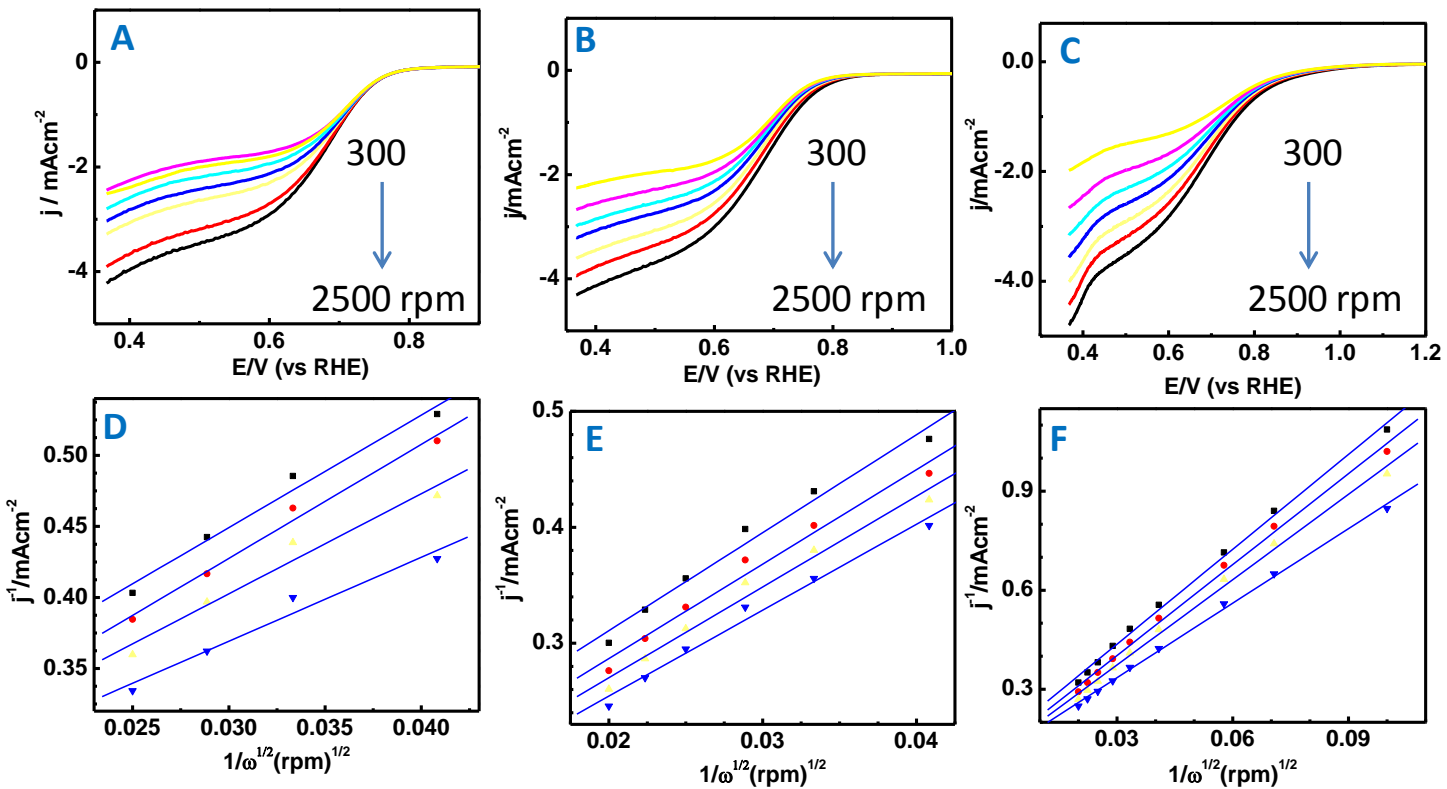


Fig. S10 LSV response for the stability of GC/MWCNT-CoTHPP (a), GC/MWCNT-CoTCPP (b), GC/MWCNT-CoTPP (c) and GC/Pt-C (d) electrodes for ORR (at 1600 rpm) in 0.1 M HClO₄ at the scan rate of 100 mVs⁻¹. Dotted lines represent the first LSV response while solid lines represent LSV response after 3000 CV cycles under the same conditions.

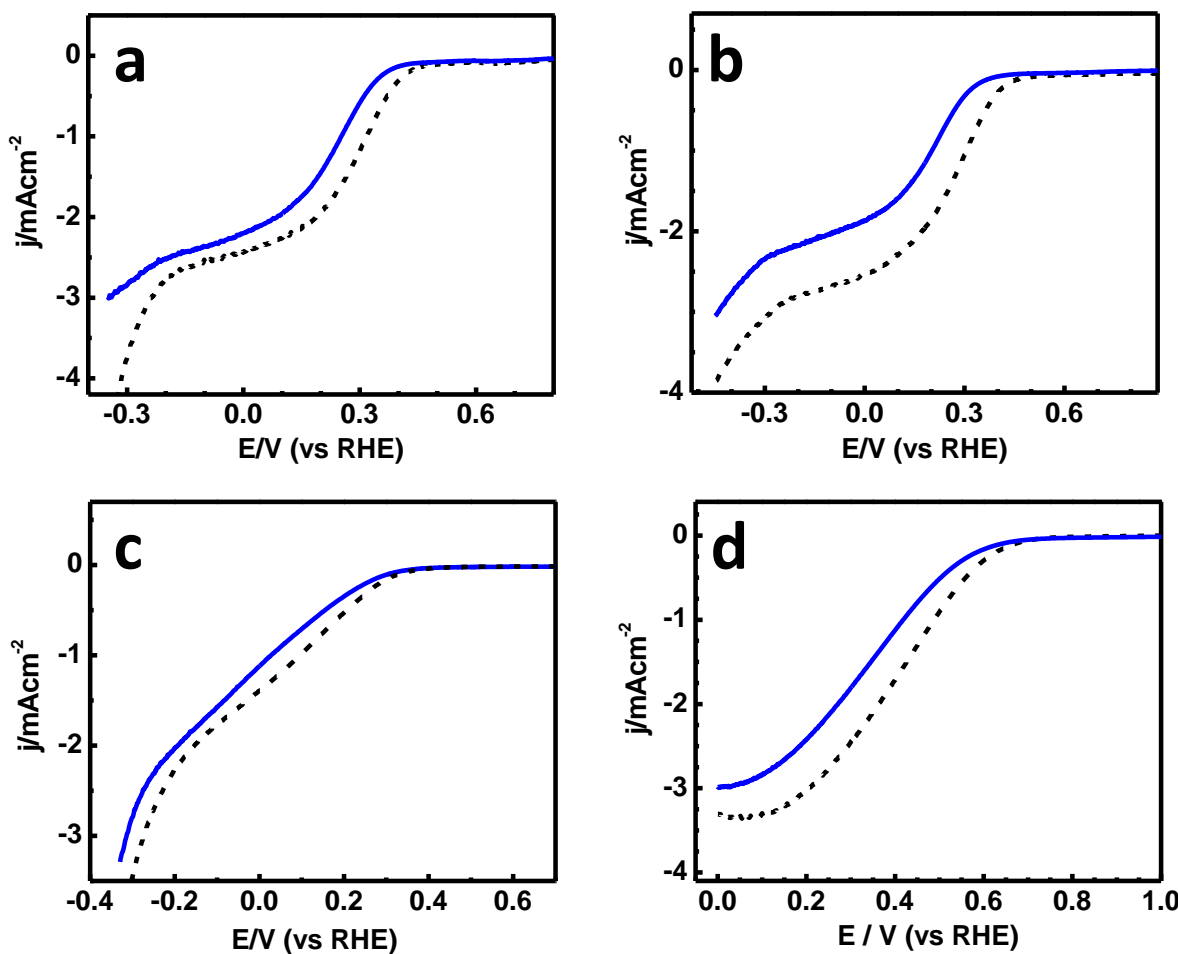


Fig. S11 XRD patterns of MWCNT-CoTHPP (A), MWCNT-CoTCPP (B) and MWCNT-CoTPP (C) on ITO plates (thin film of the respective material is coated on ITO plates) before (a, b, c) and after (a', b', c') stability test (3000 CV cycles).

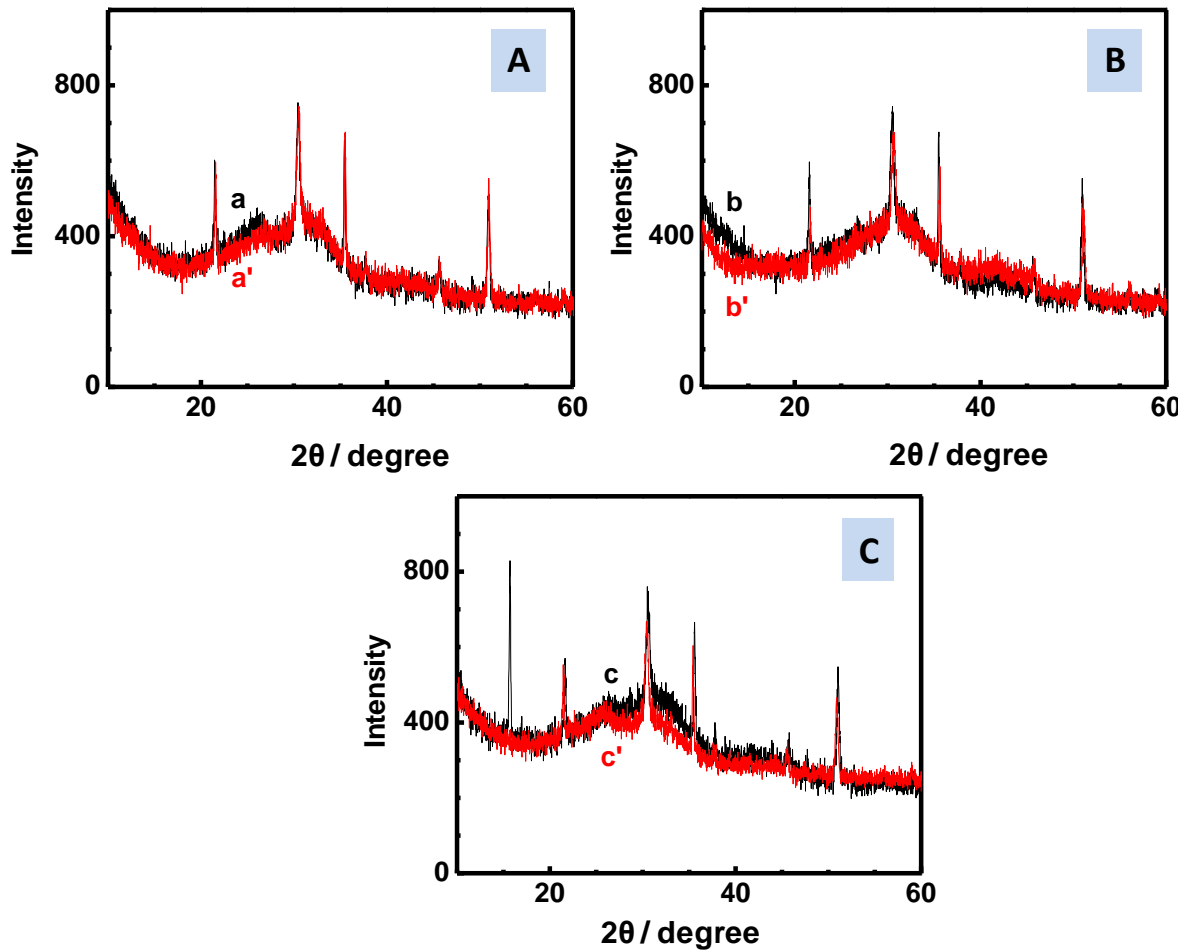


Fig. S12 SEM images of MWCNT-CoTHPP (a, a'), MWCNT-CoTCPP (b, b') and MWCNT-CoTPP (c, c') on ITO plates (thin film of the respective material is coated on ITO plates) before (a, b, c) and after (a', b', c') stability test (3000 CV cycles).

